Hunting the main player enabling *Chlamydomonas reinhardtii* growth under fluctuating light

Martina Jokel[1], Xenie Johnson[2], Gilles Peltier[2], Eva-Mari Aro[1] and Yagut Allahverdiyeva[1,*] iD

[1]*Molecular Plant Biology, Department of Biochemistry, University of Turku, Turku FI-20014, Finland, and*
[2]*Laboratoire de Bioénergétique et Biotechnologie des Bactéries et Microalgues, CEA, CNRS, Aix-Marseille Université, Institut de Biosciences et Biotechnologies Aix-Marseille, CEA Cadarache, Saint-Paul-lez-Durance F-13108, France*

SUMMARY

Photosynthetic organisms have evolved numerous photoprotective mechanisms and alternative electron sinks/pathways to fine-tune the photosynthetic apparatus under dynamic environmental conditions, such as varying carbon supply or fluctuations in light intensity. In cyanobacteria flavodiiron proteins (FDPs) protect the photosynthetic apparatus from photodamage under fluctuating light (FL). In *Arabidopsis thaliana*, which does not possess FDPs, the PGR5-related pathway enables FL photoprotection. The direct comparison of the *pgr5*, *pgrl1* and *flv* knockout mutants of *Chlamydomonas reinhardtii* grown under ambient air demonstrates that all three proteins contribute to the survival of cells under FL, but to varying extents. The FDPs are crucial in providing a rapid electron sink, with *flv* mutant lines unable to survive even mild FL conditions. In contrast, the PGRL1 and PGR5-related pathways operate over relatively slower and longer timescales. Whilst deletion of PGR5 inhibits growth under mild FL, the *pgrl1* mutant line is only impacted under severe FL conditions. This suggests distinct roles, yet a close relationship, between the function of PGR5, PGRL1 and FDP proteins in photoprotection.

Keywords: alternative electron transport, *Chlamydomonas*, flavodiiron protein, PGR5, PGRL1.

INTRODUCTION

During oxygenic photosynthesis, light-harvesting antenna complexes absorb and transfer light energy to Photosystem II (PSII) and Photosystem I (PSI). These photosystems function in series to drive electrons originating from water splitting at the PSII donor-side to reduce ferredoxin (Fd) and NADP+ at the PSI acceptor-side in a chain of reactions called linear electron transport (LET). The two photosystems are interconnected via cytochrome b_6f (Cyt b_6f) complex and plastocyanin, a small soluble protein. The LET is coupled with proton translocation across the thylakoid membrane, and the resulting *proton motive force* (*pmf*) drives ATP synthesis. NADPH and ATP, produced by photosynthesis, are used to power carbon fixation and other metabolic pathways.

Photosynthetic organisms have developed several photoprotective mechanisms and alternative electron transport pathways to maintain optimal redox poise of the photosynthetic apparatus and to fine-tune the NADPH/ATP ratio under different environmental conditions (Peltier *et al.*, 2010; Cardol *et al.*, 2011; Allahverdiyeva *et al.*, 2015a). Cyclic electron transport (CET) around PSI contributes to *pmf* formation and therefore also to ATP

synthesis without additional NADPH formation (Shikanai, 2014; Finazzi and Johnson, 2016; Shikanai and Yamamoto, 2017). In *Chlamydomonas reinhardtii*, two CET pathways around PSI are suggested: firstly, the NADPH-dependent pathway involving type II NAD(P)H-dehydrogenase (NDA2), which recycles electrons from PSI into the intersystem chain via NADPH (Jans *et al.*, 2008); and secondly, the Fd-dependent pathway, which is mediated by two proteins: PROTON GRADIENT REGULATION 5 (PGR5) and PGR5-LIKE PHOTOSYNTHETIC PHENOTYPE 1 (PGRL1) (for review, see Alric, 2010, 2014). PGR5 is a small thylakoid protein without a specific sequence motif that could predict any participation in electron transport. However, PGR5 in *Arabidopsis thaliana* was proposed to be involved in CET around PSI, thus also preventing the acceptor-side of PSI from over-reduction (Munekage *et al.*, 2002). It was later shown that, under fluctuating light (FL), PGR5 is essential (Tikkanen *et al.*, 2010) for the photoprotection of PSI by the limitation of LET via photosynthetic control at the level of Cyt b_6f in *A. thaliana* (Suorsa *et al.*, 2012). Moreover, PGRL1 and PGR5 exhibited similar expression patterns and are proposed to be in the same CET pathway

(DalCorso *et al.*, 2008; Hertle *et al.*, 2013). PGRL1 has two transmembrane domains with both the N- and C-termini of the mature protein exposed to the stroma (DalCorso *et al.*, 2008). It has been proposed that PGRL1 has the capacity to accept electrons from Fd and reduce quinones, and that PGR5 can interact with PGRL1, therefore suggesting that PGR5/PGRL1 is the ferredoxin-plastoquinone reductase, FQR (Hertle *et al.*, 2013). In *C. reinhardtii* it was shown that, under anoxic conditions, a super-complex of PGRL1, PSI-LHCI-LHCII, Fd, the Fd-NADP$^+$-oxidoreductase (FNR) and Cyt b_6f (Iwai *et al.*, 2010; Takahashi *et al.*, 2013) as well as the Ca^{2+} sensor protein (CAS) and anaerobic response 1 (ANR1) is formed and promotes CET (Terashima *et al.*, 2012). The absence of PGR5 in this PSI/Cyt b_6f CET super-complex (Iwai *et al.*, 2010; Terashima *et al.*, 2012; Takahashi *et al.*, 2013) has been attributed to its lower expression level. Nevertheless, it has been proposed that PGR5 is involved in CET around PSI in *C. reinhardtii* (Johnson *et al.*, 2014) similar to PGRL1 (Petroutsos *et al.*, 2009; Tolleter *et al.*, 2011; Dang *et al.*, 2014). In oxic conditions, a high-molecular-mass complex harbouring PGRL1, PETO and FNR, but lacking both PSI and Cyt b_6f, was suggested to act as a pre-complex for the CET super-complex (Takahashi *et al.*, 2013).

In *C. reinhardtii* the flavodiiron proteins (FDPs) FLVA and FLVB have been proposed as additional components of the photosynthetic electron transport chain, also functioning on the acceptor-side of PSI (Dang *et al.*, 2014; Allahverdiyeva *et al.*, 2015b; Jokel *et al.*, 2015; Chaux *et al.*, 2017a) and presumably using NAD(P)H as electron donor to reduce O_2 to water (Vicente *et al.*, 2002). FDPs in photosynthetic organisms consist of three distinct domains, an N-terminal β-lactamase-like domain (Fe-Fe), a flavodoxin-like domain (FMN) and a C-terminal NAD(P)H-flavin reductase-like domain (Flv). The Fe-Fe and FMN domains form the conservative core domain of FDPs, and are also found in FDPs from archaea and anaerobic bacteria where they are involved in the reduction of O_2 or NO. In contrast, the Flv domain is only found in FDPs from oxygenic photosynthetic organisms (Wasserfallen *et al.*, 1998). Previous studies in cyanobacteria showed that Flv1 and Flv3 proteins catalyse the light-dependent reduction of O_2 to water (Helman *et al.*, 2003) without reactive oxygen species (ROS) production (Vicente *et al.*, 2002). This process, also called the Mehler-like reaction, protects PSI from rapid changes in light intensity, thus enabling the growth of *Synechocystis* sp. PCC6803 and *Anabaena* sp. PCC7120 (hereafter *Synechocystis* and *Anabaena*, respectively) under FL (Allahverdiyeva *et al.*, 2013). Another cyanobacterial FDP heterodimer, encoded by the *flv4-2* operon, has been shown to be active in the photoprotection of PSII (Zhang *et al.*, 2009; Bersanini *et al.*, 2014, 2017). Genes encoding proteins with high homology to cyanobacterial Flv1 and Flv3 are present in non-vascular plants and in gymnosperms, but were lost during evolution in flowering plants (Allahverdiyeva *et al.*, 2015b; Ilík *et al.*, 2017). The crucial role of FDPs as a rapidly functioning electron sink has also been demonstrated in recent studies of the moss *Physcomitrella patens*, during exposure to FL (Gerotto *et al.*, 2016), and in the liverwort *Marchantia polymorpha*, at the onset of light exposure (Shimakawa *et al.*, 2017). The latest research by Chaux *et al.* (2017a) confirmed this important function of FDPs also in *C. reinhardtii*. Additionally, it has been shown that *P. patens* FDPs are able to function also in *A. thaliana* and rice, and that they can partially compensate for the loss of PGR5 (Yamamoto *et al.*, 2016; Wada *et al.*, 2018).

Recent works in *A. thaliana* lacking FDPs has provided valuable information about the important role of PGR5 in vascular plants under FL intensities (Tikkanen *et al.*, 2010; Suorsa *et al.*, 2012) and about the indispensable role of FDPs in cyanobacteria, which do not hold a homologous gene for *pgrl1*, but do possess a gene encoding a PGR5-like protein with a very low sequence similarity (50%) with the one in *A. thaliana* (Yeremenko *et al.*, 2005; Allahverdiyeva *et al.*, 2015b). To evaluate the degree of importance of the FDP and the PGR5/PGRL1-mediated electron transport pathways under FL conditions, we performed comparative studies on the respective knockout mutants in the model photosynthetic green alga *C. reinhardtii*, which naturally possesses all three protein types (PGR5, PGRL1 and FDPs). We conclude that all three proteins contribute to the survival of cells under FL, but to varying extents. In particular, the FDP-mediated pathway in *C. reinhardtii* is indispensable for coping with sudden increases in light intensity.

RESULTS

Growth phenotype

For the comparative analysis of the impact of the absence of PGR5, PGRL1 or FDPs on the survival of *C. reinhardtii* under FL intensities, photoautotrophically grown wild-type (wt) and the respective single mutants were exposed to different FL regimes. The *pgr5* mutant demonstrated strongly impaired growth during mild FL (FL 20/200), while *pgrl1* was not affected under such illumination conditions (Figure 1). Importantly, the complementation of PGR5 (*pgr5* c1) restored the wt 137c phenotype (Figure 1a), confirming that the impaired growth of the *pgr5* mutant was due to the absence of PGR5. The *pgrl1* mutant showed impaired growth as compared with the wt 137c only under the most severe FL (FL 20/600) condition (Figure 1b). Under this condition, the *pgr5* mutant was unable to grow (Figure 1b).

The sensitivity of the *pgrl1* mutant to severe FL conditions is in accordance with a previous study (Dang *et al.*, 2014). Importantly, the growth pattern of the *pgr5* and *pgrl1* mutants under various continuous irradiance conditions [constant light (CL) 20, high-light (HL) 200 or HL

(a)

(b)
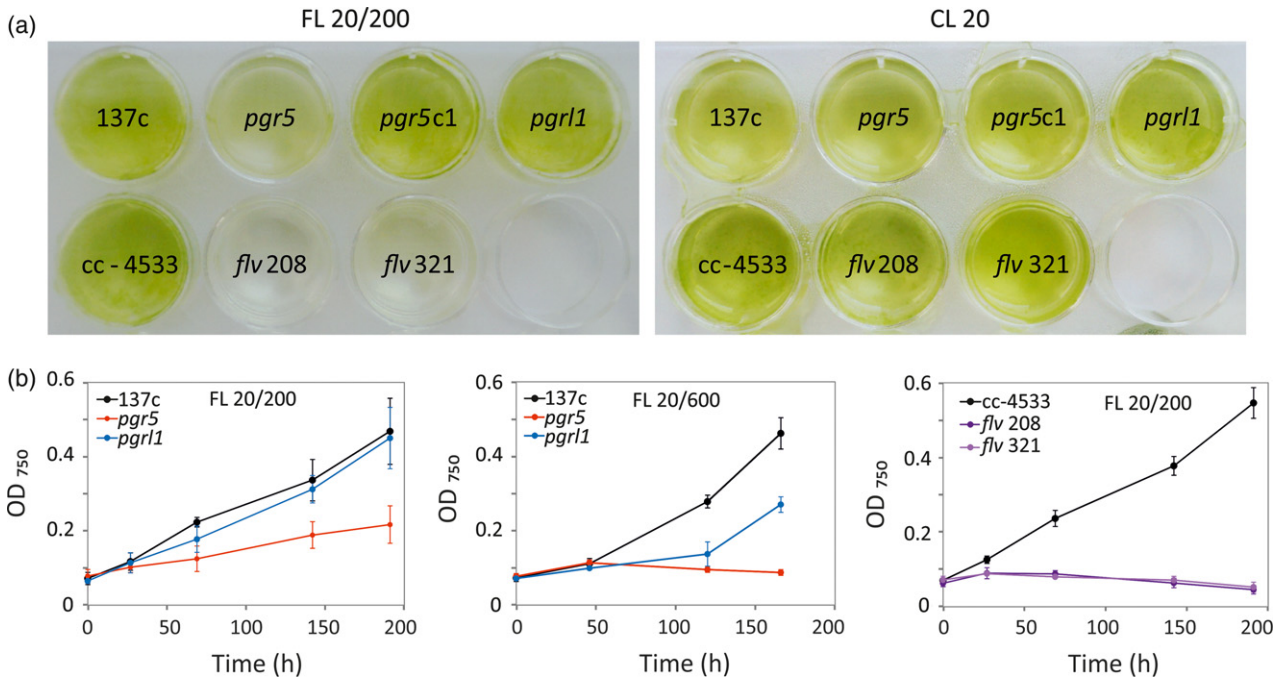
Figure 1. Growth phenotype of *Chlamydomonas reinhardtii* wild-type (wt) (137c), *pgr5*, *pgrl1* mutant, *pgr5* complementation (c1), wt cc-4533, *flv* 208 and *flv* 321 cultures.

(a) A photograph of liquid cultures grown under constant light (CL 20, 20 μmol photons m^{-2} sec^{-1}) and fluctuating light (FL 20/200, 5 min, 20 μmol photons m^{-2} sec^{-1}/30 sec, 200 μmol photons m^{-2} sec^{-1}) conditions for 7 days.

(b) Growth curves of *C. reinhardtii* wt (137c), *pgr5* and *pgrl1* cells cultivated in mild FL (FL 20/200, 5 min, 20 μmol photons m^{-2} sec^{-1}/30 sec, 200 μmol photons m^{-2} sec^{-1}) and harsh FL (FL 20/600, 5 min, 20 μmol photons m^{-2} sec^{-1}/30 sec, 600 μmol photons m^{-2} sec^{-1}) conditions. The growth curves of wt cc-4533, *flv* 208 and *flv* 321 were recorded only from mild FL 20/200 conditions. The values are the mean of four biological replicates (± SD).

600 μmol photons m^{-2} sec^{-1}] did not significantly differ from the parental wt 137c (Figure S1).

Next, the impact of the *flv* knockout on the growth performance of the cells was evaluated. The *flv* mutants were verified with polymerase chain reaction and immunoblot analysis (Figure S2). The insertion of the paromomycin resistance cassette into the *flvB* gene resulted not only in elimination of FLVB but also in the loss of FLVA, probably due to degradation and/or post-translational modifications. We selected *flv* 208 and *flv* 321 as the mutant lines missing both FDPs for further analysis. The *flv* 208 and *flv* 321 mutants died even under mild FL conditions (FL 20/200), thus demonstrating the most drastic phenotype of all studied mutants (Figure 1a and b). No significant differences were observed in the growth pattern of the *flv* mutants under constant illumination (CL 20 and CL 200) compared with the parental wt cc-4533 cells (Figure S1a and b). Strong growth retardation of the *flvB* mutant line under FL conditions was recently observed on solid agar (Chaux et al., 2017a).

Functional status of the photosynthetic apparatus of the *pgr5* and *pgrl1* mutants

The photosynthetic activity of *C. reinhardtii* wt 137c, *pgr5* and *pgrl1* cultures grown at FL 20/200 for 7 days was assessed by Chl *a* fluorescence and P700 analysis using fluctuating actinic light provided by a DUAL-PAM-100. The *pgr5* mutant demonstrated a significantly lower effective yield of PSII, Y(II), (~0.45) even during the low-light (LL; 20 μmol photons m^{-2} sec^{-1}) phase, as compared with wt 137c or the *pgrl1* mutant (both ~0.7; Figure 2a). During the HL phase, Y(II) decreased in wt 137c and *pgrl1* (to ~0.35 for both), but the most drastic decrease in Y(II) was observed in *pgr5* (to <0.15). Similarly, the effective yield of PSI, Y(I), was lower in *pgr5* cells already under the LL phase (~0.6) as compared with wt 137c or *pgrl1* (>0.75 both; Figure 2b). Upon application of the HL phase, Y(I) decreased to a much lower level (<0.1) in the *pgr5* cells compared with wt 137c and *pgrl1* (~0.2 for both). Interestingly, the PSI yield significantly increased in the wt 137c within 20 sec after the onset of the HL (~0.4, see the 2nd SP during the HL phase).

Unlike wt 137c cells, *pgr5* mutant cells could not generate donor-side limitation of PSI, Y(ND), during the short HL phase of the FL (Figure 2c). The *pgrl1* mutant did demonstrate a small Y(ND) during the first HL phase, and the difference between its Y(ND) and that of wt 137c cells became smaller with each HL phase, whereby reaching about half of the Y(ND) level of wt 137c at the third HL phase (~0.1 and ~0.2, respectively). Concomitantly the
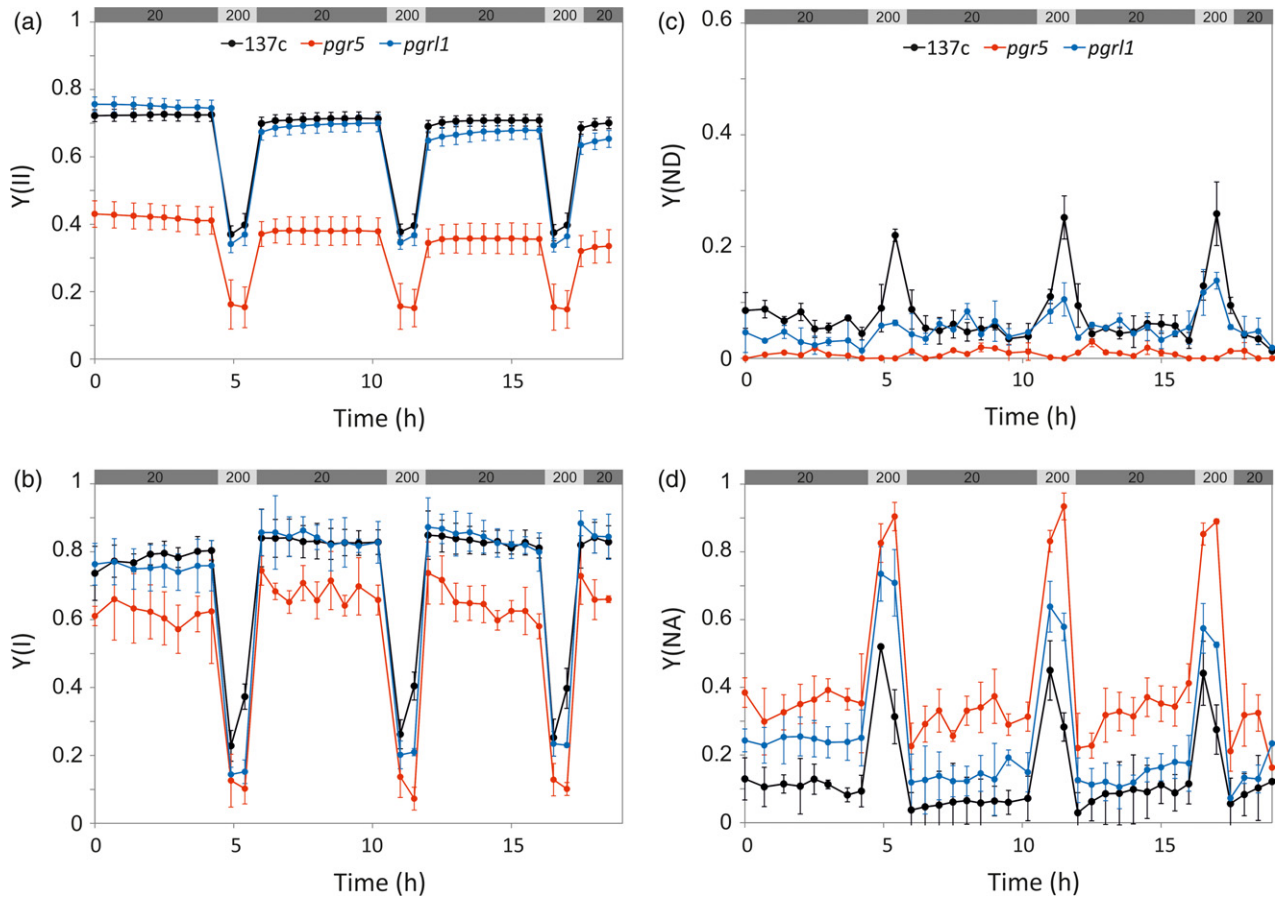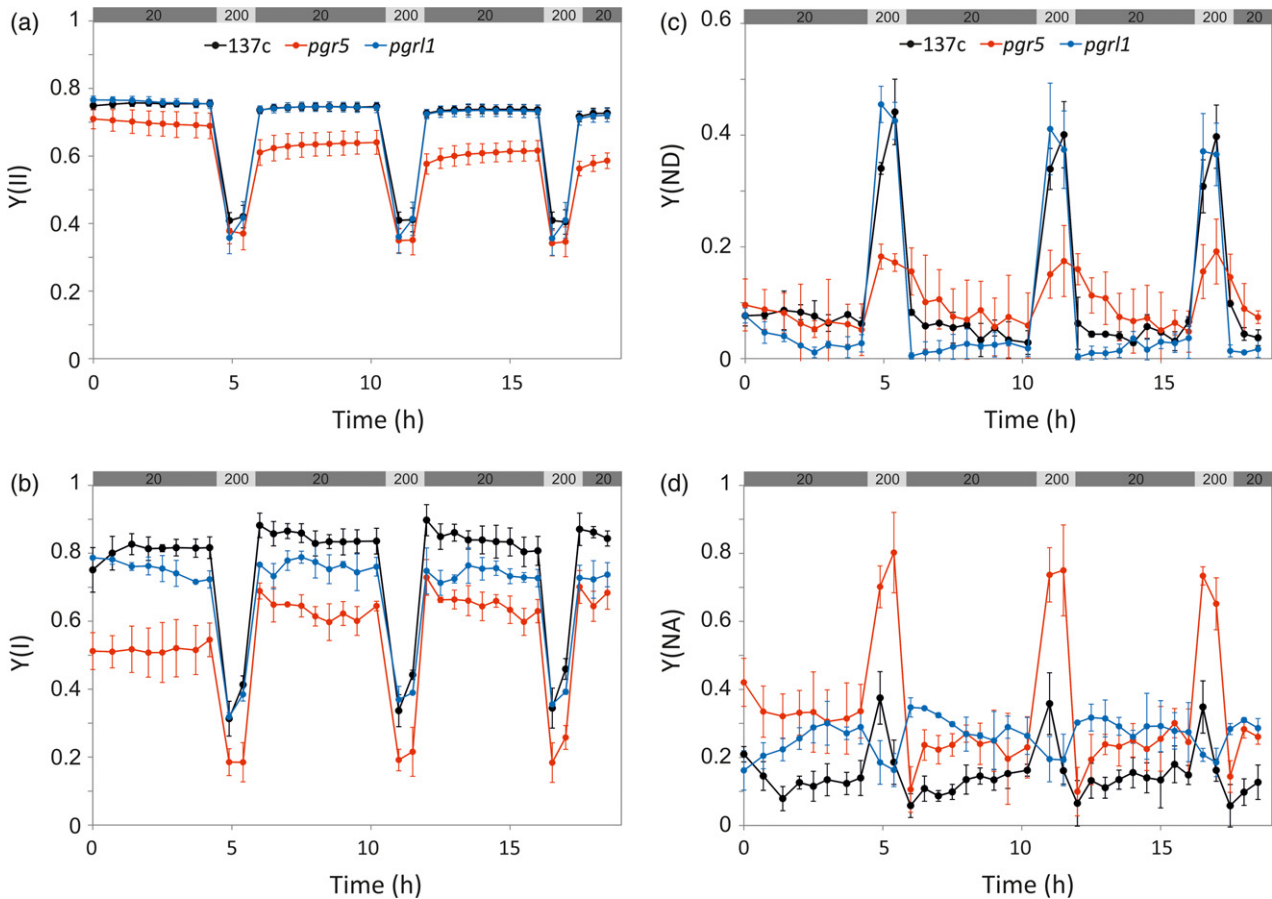
Figure 2. Photosynthetic activity after growth at fluctuating light (FL). The wild-type (wt) 137c, *pgr5* and *pgrl1* mutant cells grown under FL (FL 20/200, 5 min, 20 μmol photons m^{-2} sec^{-1}/30 sec, 200 μmol photons m^{-2} sec^{-1}) for 7 days were transferred to the DUAL-K25 quartz glass cuvette and subjected to sudden changes in actinic light intensity with a Dual PAM-100.

The effective yields of Photosystem II (PSII) (a), Photosystem I (PSI) (b), PSI donor-side limitation (c) and PSI acceptor-side limitation (d) were determined simultaneously. The values shown here are the mean of four biological replicates (±SD).

acceptor-side limitation of PSI, Y(NA), was already high (~0.35) in *pgr5* during the LL phase, and became even higher upon application of HL (~0.9) with respect to the wt 137c cells (~0.1) and the *pgrl1* mutant (~0.65; Figure 2d). The *pgrl1* cells showed an intermediate Y(NA) level (~0.6) between the *pgr5* mutant and wt 137c at both LL phase and at each HL phase of the FL 20/200 condition.

In order to understand the mechanisms behind the sensitivity to FL 20/200, we grew all mutant lines at constant low light (CL 20), and thereafter subjected the cells to sudden changes in the light intensity using DUAL-PAM and monitored simultaneously the Chl *a* fluorescence and P700 redox-changes. In contrast to the FL 20/200 grown cells, the PSII yield, Y(II), was only slightly lower in the *pgr5* mutant (~0.7) compared with the wt 137c or *pgrl1* (both ~0.75) during the LL phase, and decreased successively after each HL phase (Figure 3a). This demonstrated the accumulation of excess electrons in the intersystem electron chain of the *pgr5* mutant over time. During each HL

phase, Y(II) decreased in *pgr5*, *pgrl1* and wt 137c to similar values (~0.38). In contrast, the PSI yield, Y(I), was already significantly compromised in *pgr5* compared with wt 137c during both the LL and HL phases (Figure 3b), presenting a similar trend to that observed for the FL 20/200 grown cells. However, unlike the cells grown at FL 20/200, the *pgr5* mutant cells grown under CL could induce considerable Y(ND), which was nearly half of the values recorded for wt 137c and *pgrl1* (Figure 3c). The acceptor-side limitation of PSI, Y(NA), was high in *pgr5* as compared with the wt 137c during both the LL and HL phases (Figure 3d). The *pgrl1* cells showed similar Y(NA) as *pgr5* during each LL phase, which unexpectedly decreased to a much lower level upon application of each HL phase.

Next we monitored non-photochemical quenching (NPQ) formation by the wt 137c and mutant lines grown in constant and FL. The wt 137c cells grown at CL 20 demonstrated a much lower NPQ during the HL phase as compared with the cells grown at FL 20/200 (Figure S3b). The

Figure 3. Photosynthetic activity of the wild-type (wt) 137c, *pgr5* and *pgrl1* mutant cells grown under constant light (CL 20) for 7 days. The cells were transferred to the Dual PAM-100 and subjected to sudden changes in actinic light intensity.

The effective yields of Photosystem II (PSII) (a), Photosystem I (PSI) (b), PSI donor-side limitation (c) and PSI acceptor-side limitation (d) were determined simultaneously. The values shown here are the mean of four biological replicates (±SD).

pgr5 mutant induced only an insignificant level of NPQ upon application of the HL phase, whereas *pgrl1* demonstrated an intermediate level of NPQ between that of wt 137c and *pgr5*.

Low-temperature 77K fluorescence emission was performed to analyse possible changes in state transitions in *C. reinhardtii* wt 137c, *pgr5* and *pgrl1* lines grown at CL 20 and FL 20/200. All cells demonstrated the typical fluorescence emission peaks originating from PSII antenna pigments at shorter wavelengths (687 and 697 nm), as well as the longer wavelength fluorescence peak (at about 714 nm) from PSI antenna pigments. Both the *pgr5* and *pgrl1* mutants grown at CL (CL 20) demonstrated a slightly higher peak at 714 nm as compared with the wt 137c (Figure S4a). This suggests that the energy distribution between the two photosystems was slightly altered in favour of PSI in the *pgr5* and *pgrl1* cells grown under the CL 20 condition. The increased transition to state-2 in *pgrl1* has been reported in an earlier study (Dang *et al.*, 2014). Exposure of the cells to HL (HL 200) for 24 h induced a

relatively larger transition to state-2 in both mutants (Figure S4b). Under FL conditions, *pgrl1* demonstrated a mild state-2 phenotype, whereas the *pgr5* mutant showed a strong state-2 phenotype, similar to that observed under HL 200 (Figure S4c). This is in line with a more reduced redox status of PQ-pool in the *pgr5* mutant compared with wt or *pgrl1* grown under FL 20/200.

Functional status of the photosynthetic apparatus of *flv* mutants

The photosynthetic activity of the *flv* mutants was compared with the parental wt cc-4533 only in CL (CL 20) grown cells, as the *flv* mutants did not grow in FL 20/200 conditions. As opposed to *pgr5* and *pgrl1* grown at CL 20, the effective PSII yield, Y(II), was significantly lower in the *flv* mutants already in the LL phase, and the difference between wt cc-4533 and the *flv* mutants dramatically increased upon application of the HL phase (Figure 4a). The effective PSI yield, Y(I), of wt cc-4533 and the *flv* mutants did not differ significantly during the LL phases (Figure 4b).
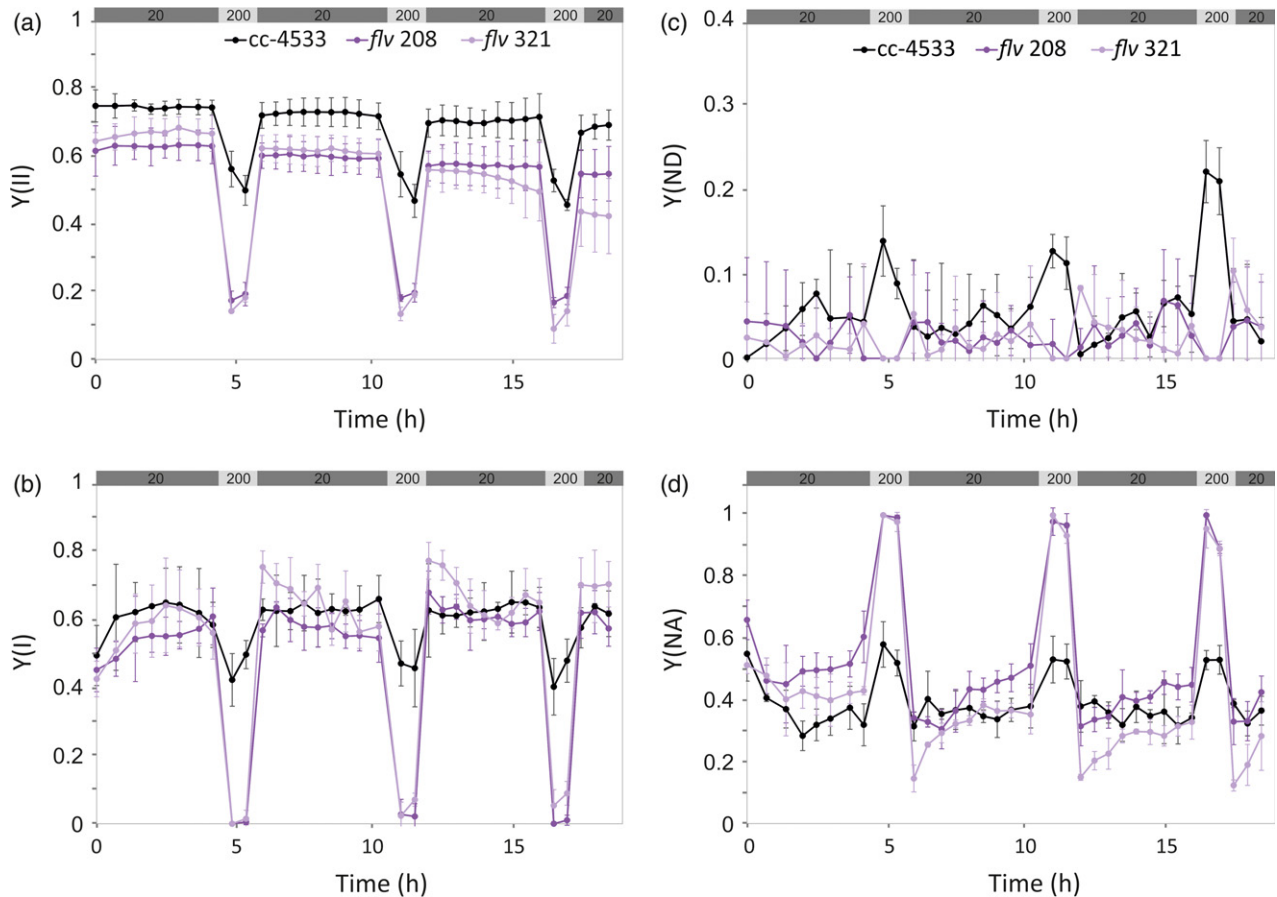
Figure 4. Photosynthetic activity of wild-type (wt) cc-4533 (cw15 mt-), *flv 208* and *flv 321* mutant cells grown under constant light (CL 20, 20 μmol photons m^{-2} sec^{-1}) for 7 days. The cells were transferred to the DUAL-K25 quartz glass cuvette and subjected to sudden changes in actinic light intensity.
The effective yields of Photosystem II (PSII) (a), Photosystem I (PSI) (b), PSI donor-side limitation (c) and PSI acceptor-side limitation (d) were detected simultaneously. The values shown here are the mean of three biological replicates (±SD).

However, upon application of HL, Y(I) of wt cc-4533 reduced only slightly, while the *flv* mutants demonstrated a dramatic decline in Y(I). This was accompanied by a severe acceptor-side limitation of PSI, Y(NA), in the *flv* mutants during the HL phase as compared with wt cc-4533 (Figure 4d). Accordingly, the *flv* mutants did not show any significant donor-side limitation of PSI, Y(ND), while wt cc-4533 did establish a low Y(ND) during HL (Figure 4c). Moreover, the induction and relaxation of NPQ was slower, therefore the NPQ peak was delayed during the HL phases in the *flv* mutants, compared with the wt cc-4533 (Figure S3c). The low-temperature fluorescence emission showed that the *flv* mutants grown in CL 20 were mostly in state-2 compared with wt cc-4533 cells (Figure S4d).

Next we monitored fast P700 redox kinetics of dark-adapted *C. reinhardtii* wt and mutant cells (cultivated under CL 20) at the onset of light. The wt cc-4533 and wt 137c cells showed characteristic waves in P700 kinetics: a fast P700 oxidation followed by its re-reduction and re-oxidation during the first seconds of illumination (Figure 5).

The lack of a fast re-oxidation rise of the P700 signal is another indicator of acceptor-side limitation of PSI, and was observed previously in the *flv1* and *flv3* mutants of *Synechocystis* (Helman *et al.*, 2003; Allahverdiyeva *et al.*, 2013), and in *A. thaliana*, which naturally lacks FDPs (Ilík *et al.*, 2017). Therefore, the fast re-oxidation rise, within 1 sec, has been attributed to the function of FDPs (Ilík *et al.*, 2017). As expected, *C. reinhardtii flv* 208 and *flv* 321 mutant lines were missing the characteristic P700 re-oxidation rise (Figure 5). Moreover, the P700 signal dropped below its initial dark level and remained negative during the 5 sec of illumination, presumably due to the accumulation of reduced Fd in the absence of FDPs. A similar trend was observed in the wt cc-4533 line under anoxic conditions. This, together with the data demonstrating interaction of Fdx1 and FLVB (Peden *et al.*, 2013), strongly suggests that the electron donor for FDPs is Fd rather than NAD(P)H. Interestingly, the P700 re-oxidation rise was also strongly reduced in *pgr5*, yet the *pgrl1* mutant showed a similar pattern to wt ccc 137c cells. This result suggests
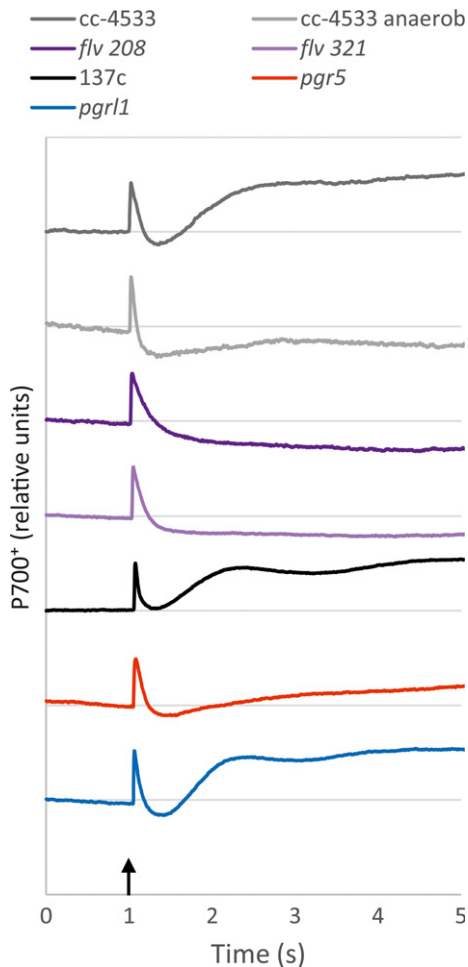
Figure 5. P700 oxido-reduction kinetics at onset of light. The wild-type (wt) 137c, *pgr5*, *pgrl1*, wt cc-4533, *flv* 208 and *flv* 321 lines were grown under constant light (CL 20), and dark-acclimated for 45 min prior to the experiment. The black arrow indicates switching on light (1000 μmol photons m^{-2} sec^{-1}). The curves are representative of four biological replicates.

that the loss of PGR5 creates a fast acceptor-side limitation in the mutant due to high electron traffic from Cyt b_6f, or that FDPs are not actively functioning in the Mehler-like reaction in *pgr5* lines.

Accumulation of photosynthetic and respiratory proteins

Immunoblot analysis of several proteins involved in photosynthesis and respiratory processes was performed on *C. reinhardtii* wt 137c, *pgr5* and *pgrl1* cells grown for 7 days under CL 20 and FL 20/200 regimes. Accumulation of proteins representing PSII (PsbA) and PSI (PsaA) complexes did not differ significantly between *pgr5*, *pgrl1* and the wt 137c grown under the CL 20 condition (Figure 6a). Both the *pgr5* and *pgrl1* mutants grown under the FL 20/200 condition demonstrated a slight decrease in PsbA (D1) amounts compared with wt 137c cells. The *pgr5* mutant showed a strong decrease in the amount of the PsaA

subunit of the PSI complex (~5 times less than wt), whereas PsaA accumulation was unaffected in the *pgrl1* line. However, the *pgrl1* mutant demonstrated a strong decrease in abundance of the Cyt *f* subunit of the Cyt b_6f complex, compared with wt 137c cells. This was observed under both CL 20 and FL 20/200 conditions, and was more pronounced under the latter condition (~half of the wt 137c). The *pgrl1* results contrasted those of the *pgr5* mutant, which did not show a substantial change in Cyt *f* accumulation.

The PGRL1 protein was similarly accumulated in wt 137c and *pgr5* lines under CL 20 conditions, and a slight upregulation of PGRL1 was observed in the *pgr5* mutant under the FL 20/200 condition (Figure 6a). The PGR5 protein was not detectable in the membrane extracts of either the *pgr5* or *pgrl1* mutant cultures. Similar findings have been reported previously for *pgr5* and *pgrl1* lines in *A. thaliana* and *C. reinhardtii* (DalCorso *et al.*, 2008; Johnson *et al.*, 2014). Nevertheless, it is possible that PGR5 in the *pgrl1* mutant was below the limit of detection of immunoblotting (Steinbeck *et al.*, 2015) or not detected due to its accumulation in soluble-form, without PGRL1 acting as an anchor-protein. Unfortunately, in our experimental conditions the α-PGR5 antibody did not recognize the PGR5 protein in whole-cell extracts of *C. reinhardtii*, therefore we were unable to verify the possibility of free-form PGR5 in the *pgrl1* mutant. It is worth mentioning that the wt level *pgr5* transcript observed in the *pgrl1* mutant (Table S1) supports the presence of free-form PGR5 protein in the *pgrl1* mutant. In the *pgr5* mutant, the PGRL1 protein was accumulated to wt levels. The accumulation of the chloroplastic NDA2, involved in PGR5-independent CET, was not affected in *pgr5* under CL 20 or FL 20/200. However, the NDA2 protein was slightly downregulated in *pgrl1* under the FL 20/200 regime.

Light-harvesting complex stress-related protein 3 (LHCSR3), which is known as the effector protein of qE, the fastest component of NPQ, was barely detectable in both mutants grown under the CL 20 regime. However, under the FL 20/200 condition, *pgrl1* accumulated about 30% of LHCSR3 observed in the wt 137c cells, whereas LHCSR3 was still lacking in *pgr5*. This finding is in line with NPQ data (Figure S3a and b) showing that *pgr5* cannot create NPQ and that *pgrl1* has a reduced NPQ as compared with wt 137c.

Proteins located downstream of PSI were mostly upregulated under CL 20 conditions in *pgr5* and *pgrl1* (Figure 6a). FDX1 (PETF), a major ferredoxin in chloroplasts shuttling electrons between PSI and FNR, was greatly upregulated in both mutants relative to wt 137c under CL 20, whereas under FL 20/200, levels were only slightly higher. RuBisCo (RbcL) was upregulated in *pgr5* grown in CL 20, and an even higher level was observed in FL 20/200 grown cells. However, RbcL was slightly downregulated in

Figure 6. Immunoblot analysis of selected proteins from *Chlamydomonas reinhardtii* wild-type (wt) and mutant lines.
(a) The wt 137c, *pgr5* and *pgrl1* mutant lines were grown under constant illumination (CL 20, 20 μmol photons m^{-2} sec^{-1}) or fluctuating light conditions (FL 20/200, 5 min, 20 μmol photons m^{-2} sec^{-1}/ 30 sec, 200 μmol photons m^{-2} sec^{-1}).
(b) wt cc-4533, *flv 208* and *flv 321* cells were grown at CL 20 for 7 days. The western blots shown here are representative of at least three biological replicates.
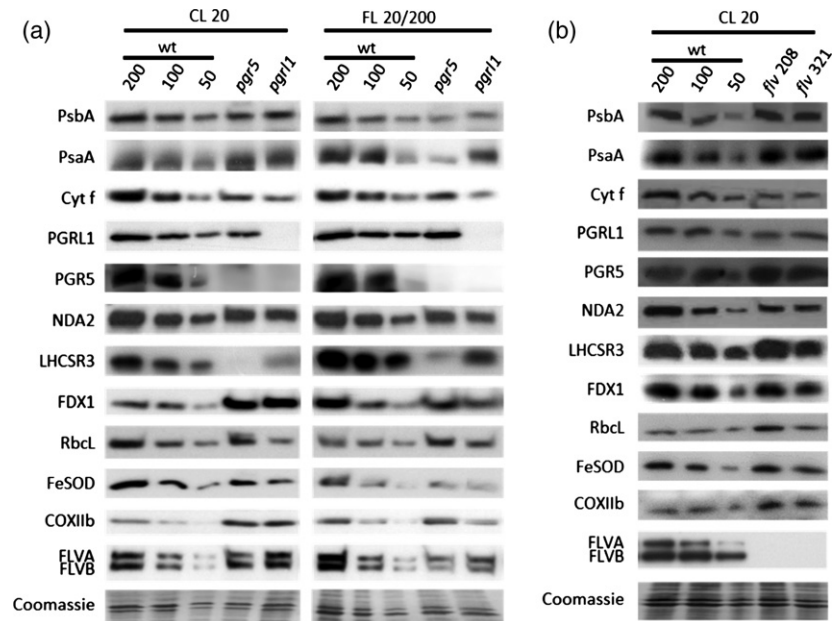
the *pgrl1* mutant grown in CL 20 conditions but slightly upregulated under FL 20/200 conditions. The FLVA and FLVB proteins were upregulated in *pgrl1* (Figure 6a) and *pgr5* grown under CL 20. The situation was different in the mutant cells grown under FL 20/200 illumination. Both mutants demonstrated FLVA levels that did not differ from wt 137c, and FLVB levels were actually slightly lower than those in wt 137c cells. This decrease of FDPs under conditions causing elevated redox-pressure has previously been reported in Dang *et al.* (2014) and is explained by the stimulation of the true Mehler-reaction, where electrons are shuttled to O$_2$ directly from PSI.

Next we studied other O$_2$-consuming pathways that could function as an electron exit in the cell. The FeSOD accumulation was not altered in the *pgr5* mutant, but was downregulated in *pgrl1* under both illumination conditions. The increase in accumulation level of COXIIb strongly suggests that the mitochondrial respiration capacity is increased in both mutants under the CL 20 condition. Under FL 20/200, the upregulation of COXIIb was less pronounced in *pgr5*, and there was no upregulation in *pgrl1* as compared with wt 137c.

Because the *flv* mutants did not grow at all under FL 20/200 conditions, only the mutant cells grown in CL (CL 20) were subjected to immunoblotting analysis. PSII (PsbA) and PSI (PsaA) core proteins and RbcL were similar or slightly upregulated in the *flv* mutant compared with the wt cc-4533, whereas Cyt *f* was downregulated (Figure 6b). However, and as opposed to the *pgr5* and *pgrl1* mutants, the accumulation of FDX1 was not significantly altered. The lack of FDPs affected other O$_2$-consuming processes, with FeSOD and COXIIb demonstrating increased accumulation in the *flv* mutants. Contrasting the results of *pgr5*

and *pgrl1* cells grown at CL 20, the LHCSR3 level was elevated in the *flv* mutants. This is in line with the results showing similar NPQ induction in the *flv* and wt cc-4533 cells during HL phases (Figure S3c). The CET-related protein NDA2 did not change its accumulation level. Interestingly, PGR5 and PGRL1 were differently regulated in the *flv* cells; PGR5 increased, whereas PGRL1 slightly decreased during the growth at CL 20 (Figure 6b).

To understand the mechanistic basis behind the different responses of *pgr5* and *pgrl1* to FL 20/200, we profiled the wt 137c and mutant transcriptomes using next-generation RNA sequencing (RNAseq) analysis. Genes that were differentially expressed a minimum of log2 fold ($P < 0.05$) in the mutants compared with the control were collected and evaluated for possible roles in FL 20/200 response. The *pgr5* cells displayed 31 down- and 38 upregulated (total 69) genes compared with the control (Table S1), whilst the *pgrl1* mutation led to the downregulation of 26 and upregulation of 38 genes from a total of 64 (Table S1). Among the differentially expressed transcripts, 19 were categorized as 'hypothetical' or 'unknown' in *pgr5*, and nine in the *pgrl1* mutant. No significant changes were observed in the *pgr5* transcript abundance in the *pgrl1* mutant, and vice versa. Importantly, only eight genes were commonly regulated in *pgr5* and *pgrl1* mutants compared with the control cells. No commonly regulated photosynthesis genes were identified in *pgr5* and *pgrl1*.

Deletion of *pgr5* resulted in a coordinated downregulation of photosynthesis-related genes, including the *PSAH* subunit of PSI complex. Moreover, the *LHCBM9*, *LHCBM7* and *LHCBM6* genes, which are known to be redox-regulated by the NAB1 repressor protein (Wobbe *et al.*, 2009), were downregulated. These genes are part of the

photosynthesis-associated nuclear genes (PhANG) expression system. Interestingly, *CURT1*, which is an evolutionarily conserved family of proteins that oligomerize thylakoid membranes, (Armbruster *et al.*, 2013; Heinz *et al.*, 2016), was downregulated, suggesting a possible modification of the thylakoid architecture in the *pgr5* mutant. Indeed, transmission electron microscopy (TEM) of the FL 20/200 grown cells revealed a less curved and looser thylakoid architecture in *pgr5* compared with wt 137c and *pgrl1* (Figure S5).

Contrasting *pgr5* results, the *pgrl1* mutant demonstrated an upregulation of several photosynthesis-related genes (Table S1). The transcript abundance of genes encoding FDX1; PETM, a nuclear-encoded Cyt b_6f subunit presumably functioning in signalling (Schneider *et al.*, 2001); and FAO5, coding for a lycopene-β-cyclase involved in carotenoid synthesis, were upregulated. Of the genes involved in carbon metabolism, FBA3 was upregulated in both *pgr5* and *pgrl1* mutants compared with the control. However, the TEM showed reduced pyrenoid formation in *pgr5* cells under FL 20/200 conditions, unlike in wt 137c and *pgrl1* lines (Figure S5).

Differently to *pgr5*, the *pgrl1* mutant showed less regulation of PhANG type genes. This correlates with the availability of other compensatory mechanisms to generate the proton gradient and reduce the PSI acceptor-side limitation under FL. Indeed, another mitochondrial gene encoding prohibitin, which is involved in mitochondrial biogenesis and protection against stress (Ahn *et al.*, 2006), was highly upregulated, providing support for compensation mechanisms at the level of respiration (Dang *et al.*, 2014).

DISCUSSION

Organisms performing oxygenic photosynthesis use solar energy and water to produce reducing equivalents and ATP in the thylakoid membrane needed for driving CO_2 assimilation and cell metabolism. Sudden exposure of these organisms to HL intensities leads to a build up of excess electrons on the redox carriers of the thylakoids producing undesired side products, like ROS, which have a signalling role (Foyer and Noctor, 2009), but also a potential to lead to photodamage. In order to maintain balanced light absorption and energy utilization under HL conditions, photosynthetic organisms have developed photoprotective mechanisms and efficient electron sinks. Particularly in aquatic environments, photosynthetic microorganisms experience drastic fluctuations in light intensity due to the lens effect of waves, shading caused by clouds and turbulences (Iluz *et al.*, 2012). Consequently, the photosynthetic apparatus of aquatic phototrophs requires rapid fine-tuning. It has been demonstrated that FDPs are responsible for survival under FL in cyanobacteria (Allahverdiyeva *et al.*, 2013), *P. patens* (Gerotto *et al.*, 2016) and in *C. reinhardtii* (Chaux *et al.*, 2017a). In contrast,

in *A. thaliana*, which lacks the genes encoding FDPs (Peltier *et al.*, 2010; Allahverdiyeva *et al.*, 2015a), the PGR5 protein safeguards the photosynthetic apparatus (Tikkanen *et al.*, 2010; Suorsa *et al.*, 2012; Tiwari *et al.*, 2016). Unlike cyanobacteria or flowering plants, the green alga *C. reinhardtii* and mosses possess the genes encoding all three proteins proposed to be involved in FL photoprotection: FDPs, PGR5 and PGRL1. It has been shown that in *C. reinhardtii* PGRL1 is involved in photoprotection under FL (Dang *et al.*, 2014). The functional interplay of all these three proteins has not been studied before. In this study, independently from Chaux *et al.* (2017a), we performed a comparative analysis of *C. reinhardtii flv*, *pgr5* and *pgrl1* knockout mutants to evaluate the relative impact of these alternative electron pathways in photoprotection under FL. The obtained data demonstrate that all three proteins of *C. reinhardtii* are important for survival under FL, but to differing extents. The cells lacking functional FDPs are unable to survive under mild FL 20/200 light, while the *pgr5* knockout mutant grows under such conditions but at a lower rate (Figure 1). The growth of the *pgrl1* mutant is affected only under very harsh FL conditions, i.e. FL 20/600.

FDPs provide a fast and strong electron sink during the first seconds after the onset of HL and contribute to the rapid induction of NPQ in *C. reinhardtii*

The function of the Flv1(A) and Flv3(A) proteins in cyanobacteria (*Synechocystis* and *Anabaena*; Allahverdiyeva *et al.*, 2013) and the FLVA and FLVB proteins in the moss *P. patens* (Gerotto *et al.*, 2016) and in *C. reinhardtii* (Chaux *et al.*, 2017a) as an electron sink is most prominent during the shift from LL to HL within a time range of minutes. In this study, we used P700 redox kinetics to observe the rapid functioning of FDPs in dark-adapted cells as electron sink downstream of PSI (Figure 5). The *flv* mutants of *C. reinhardtii* show a complete block of the PSI acceptor-side during the HL phase of the FL 20/200 light (Figure 4d), suggesting that FDPs are responsible for rapidly capturing the majority of the electrons leaving PSI during the first seconds of a HL phase. We therefore propose that in *C. reinhardtii* FDPs work as immediate electron sink, operating before any other electron transport route and relieving the sudden HL-induced electron pressure. In line with this, the high accumulation of FLVA and FLVB proteins in the *pgrl1* mutant grown under CL 20 conditions is accompanied by low PSI acceptor-side limitation, Y(NA), during HL phases (Figure 3d). This also confirms that *C. reinhardtii* FDPs can increase their O_2 photoreduction capacities under HL intensities, similar to cyanobacterial FDPs (Allahverdiyeva *et al.*, 2013).

The question arises why the PGR-mediated pathway cannot replace the lack of FDPs under FL conditions. Perhaps the main reason is the difference in the induction

time between the FDP-mediated electron sink and the PGR-mediated process. Activity of CET is modulated by the availability of Ca^{2+} (Terashima *et al.*, 2012) and redox-controlled (Takahashi *et al.*, 2013) via the thioredoxin (TRX) system (Hertle *et al.*, 2013). The switch to a high CET-state under oxic conditions is likely to be slower, as the activation of PGRL1 (PGRL1 homodimer to monomer conversion) by TRX demands high levels of reduced Fd, possibly requiring several seconds at the onset of HL illumination (Hertle *et al.*, 2013). FDPs, however, function as a rapid electron sink, interacting with the substrate, presumably reduced Fd, within a second.

It is important to note that FDPs trigger a safe water–water cycle, without intermediate ROS production (Vicente *et al.*, 2002), which contributes to the generation of *pmf* at the onset of the HL illumination (Allahverdiyeva *et al.*, 2013; Gerotto *et al.*, 2016; Chaux *et al.*, 2017a). Acidification of the lumen in turn activates another important photoprotective process, qE, which dissipates excess light energy (Horton *et al.*, 1994; Müller *et al.*, 2001; Niyogi and Truong, 2013). In green algae, LHCSR3 (Peers *et al.*, 2009) and PsbS (Correa-Galvis *et al.*, 2016) are the major qE effectors mediating energy dissipation under environmental stresses like HL and also nutrient starvation (Finazzi and Minagawa, 2015). Indeed, NPQ induction is delayed in the *flv* mutants during HL phases (Figure S3c), even though the *flv* mutants accumulate LHCSR3 at similar levels to wt cc-4533 (Figure 6b). This could indicate that, in the *flv* mutants, the generation of ΔpH is only slowed down in the beginning of the HL phase, but can reach higher levels after other processes like PGRL1-Fd-mediated CET begin functioning. Indeed, Chaux *et al.* (2017a) showed that after 3 min of illumination the NPQ of the *flv* mutant reached wt levels.

The PGR5 and PGRL1 proteins do not have a univocal relationship

In *A. thaliana*, PGRL1 has been proposed to function both as FQR and as a redox sensor (Hertle *et al.*, 2013). This may happen in cooperation with PGR5, as PGR5 can interact with PGRL1 in a redox-dependent manner. However, PGRL1 is also stable in the absence of PGR5 (DalCorso *et al.*, 2008; Hertle *et al.*, 2013; Johnson *et al.*, 2014). The interaction of PGRL1 and PGR5 possibly enhances PGRL1-Fd-mediated CET under certain conditions, i.e. anoxia, in *C. reinhardtii*. Furthermore, it was shown that PGR5 and PGRL1 are directly or indirectly involved in the attachment of FNR to the thylakoid membrane and, thus, have an effect on the modulation of electron transport downstream of PSI (Mosebach *et al.*, 2017). The *pgr5* mutant of *C. reinhardtii* has phenotypic characteristics that are nearly identical to the characteristics shown for *pgrl1* (Petroutsos *et al.*, 2009; Tolleter *et al.*, 2011; Johnson *et al.*, 2014). Nevertheless, there are several conditions when a significant

difference between the *pgr5* and *pgrl1* mutants has been observed. In *C. reinhardtii* PGRL1 has been shown to be involved in CET under oxic and anoxic conditions (Tolleter *et al.*, 2011; Terashima *et al.*, 2012), whereas the possible involvement of PGR5 in CET has been demonstrated only under anoxic conditions or in oxic conditions in specific mutants, like RuBisCO-less mutants, experiencing strong acceptor-side limitation (Alric, 2014; Johnson *et al.*, 2014). Under oxic conditions, the similar CET rates in the wt and *pgr5* mutant lines (Johnson *et al.*, 2014) suggest that NDA2-mediated CET could be the dominant route and that PGR5 is not an essential part of the PGRL1-Fd-mediated CET under normal oxic conditions (Alric *et al.*, 2010).

Our data demonstrate significant differences between the *pgr5* and *pgrl1* mutants under a FL regime. The *pgr5* mutant is impaired in growth under FL 20/200 where the *pgrl1* mutant is able to grow in a similar manner to wt 137c (Figure 1). Moreover, the photosynthetic performance of *pgr5* is strongly affected (Figure 2), even under CL 20 conditions (Figure 3). The strong phenotype observed for *pgr5* cannot be simply attributed to the lack of PGRL1-Fd-mediated CET, as the *pgrl1* mutant can cope with mildly FL (FL 20/200) in a similar way to wt 137c cells (Figures 1 and 2). Unchanged NDA2 levels in the *pgr5* and *pgrl1* mutants compared with wt 137c (Figure 6a) suggest that the NDA2-mediated CET probably does not compensate for the loss of these proteins.

In *pgrl1*, a high accumulation of FDPs and downregulation of Cyt *f* safeguards the PSI complex from sudden changes in light intensities (Figure 6a). During the HL phase applied to the *pgrl1* mutant grown at CL 20, limited electron transport from Cyt b_6f creates a stronger PSI donor-side limitation (Figure 3c), and a strong FDP-mediated electron sink eliminates the PSI acceptor-side limitation (Figure 3d). During growth in FL 20/200, the *pgrl1* cells accumulate relatively lower levels of FDPs as compared with CL 20 grown cells. Subsequently, application of a HL phase induces slightly higher PSI acceptor-side limitation, Y(NA), compared with the wt 137c. It is likely that under more challenging conditions (FL 20/600), the *pgrl1* cells are unable to balance the photosynthetic electron transport via PSI, resulting in strongly compromised growth (Figure 1).

In contrast to *pgrl1*, the *pgr5* mutant accumulated Cyt *f* at levels similar to that of the wt 137c (Figure 6a). The *pgr5* mutant has no donor-side limitation but large acceptor-side limitation (Figures 2c and 3c), suggesting that without PGR5, *C. reinhardtii* is unable to induce strong photosynthetic control, and consequently cannot adjust the electron pressure at the donor-side of PSI. It is striking that whilst FDPs are present in *pgr5* under both growth conditions (Figure 6a) and their O_2 photoreduction activity seems to be higher than in wt (Steinbeck *et al.*, 2015), apparently FDPs are still not able to provide enough strong sink to

overcome the strongly elevated electron traffic to PSI and oxidize P700 as rapidly as in wt or *pgrl1* (Figure 5). However, a recent study demonstrated that the heterologous expression of *P. patens* FDPs in the *A. thaliana pgr5* mutant at least partially rescued the phenotype (Yamamoto *et al.*, 2016). Nonetheless, it is highly possible that the regulatory mechanisms are different in *A. thaliana*, which does not naturally possess genes encoding FDPs. It is possible that the activity of FDPs in their endogenous environment is redox-controlled via one or two fully conserved cysteines and four cysteines that are conserved either in the FLVA or FLVB cluster (Figure S6). Such a redox regulation of FDPs may be disturbed in the *pgr5* mutant, which exhibits a more reduced status of the stromal components under FL 20/200 (Figure S4c).

Unlike *pgrl1*, which accumulated low levels of LHCSR3 compared with the wt 137c (Figure 6a; Tolleter *et al.*,

2011), *pgr5* either completely lacked (CL 20) or accumulated only trace amounts (FL 20/200; Figure 6a) of LHCSR3. In addition, *pgr5* demonstrated decreased levels of the *LHCSR3* transcript at the FL 20/200 conditions (Table S1). This was reflected in a deficiency of NPQ induction during the HL phases (Figure S3a). The fact that the LHCSR3 level is higher in *pgrl1* but not in *pgr5* supports the stronger phenotype observed in *pgr5*, and suggests somewhat complementary mechanisms of LHCSR3 and PGRL1 (Kukuczka *et al.*, 2014; Chaux *et al.*, 2017b). The accumulation of LHCSR3 in *C. reinhardtii* is controlled by a blue-light photoreceptor under HL conditions (Petroutsos *et al.*, 2016) and requires active photosynthesis (Petroutsos *et al.*, 2011; Maruyama *et al.*, 2014). Additionally, Ca^{2+} signalling via CAS is critically involved in the regulation of the HL response, particularly in the control of LHCSR3 expression (Petroutsos *et al.*, 2011). Although the *cas* transcript level
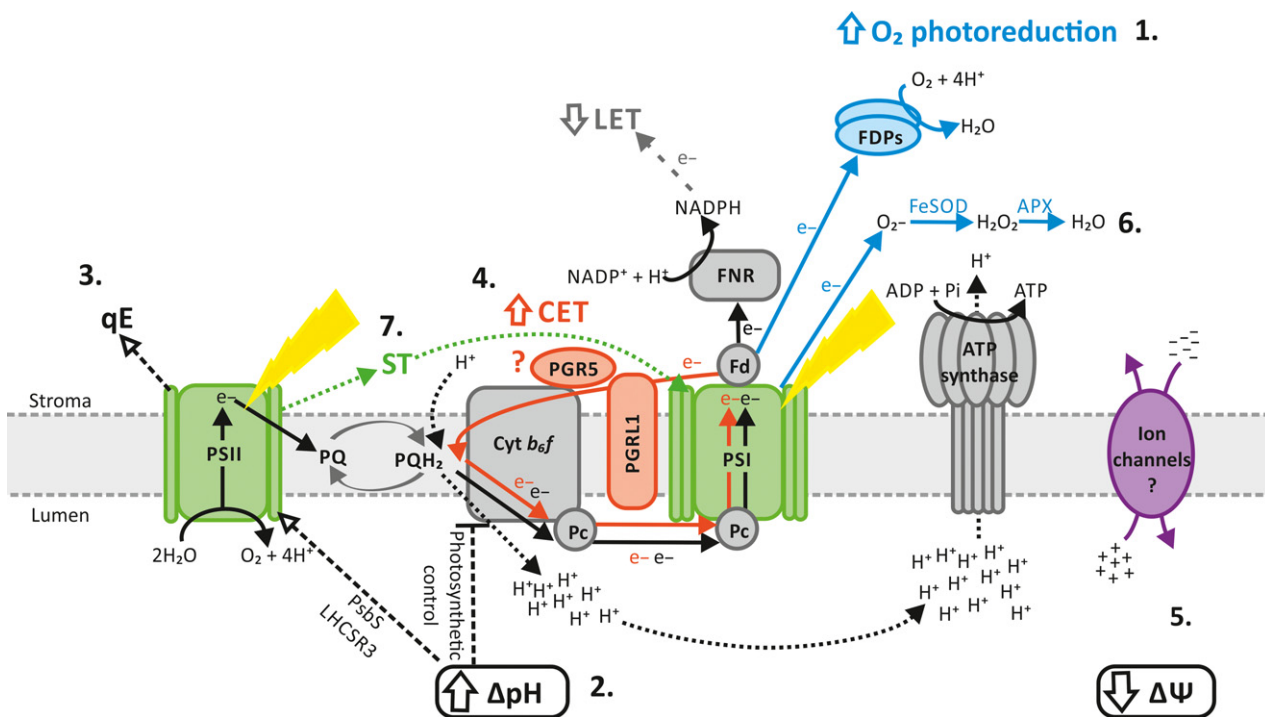
Figure 7. Schematic presentation of photosynthetic and alternative electron transport showing the occurrence of events during a shift from low-light (LL) to high-light (HL) in *Chlamydomonas reinhardtii*. Linear electron transport (LET) from H_2O to $NADP^+$ is marked by black arrows. The cyclic electron transport (CET) around Photosystem I (PSI), via the PGRL1-Fd-mediated pathway, is specified by red arrows. Blue arrows specify the O_2 photoreduction processes, mediated by flavodiiron proteins (FDPs) or the true Mehler-reaction. The latter depends on O_2 reduction at PSI, and the resulting reactive oxygen species (ROS) is scavenged by the superoxide dismutase (FeSOD) and ascorbate peroxidase (APX). FDPs mediate the direct reduction of O_2 to H_2O without the production of ROS, using reduced Fd as a donor. CET and the O_2 photoreduction processes contribute to the generation *pmf*. When *C. reinhardtii* cells undergo a sudden increase in light intensity, several processes are brought into motion at different time-scales. Our data suggest that FDPs form a strong and rapid (within 1 sec) electron sink, working immediately at the onset of HL (Figure 5). This process supports LET and contributes to the total *pmf* (2). The increase of ΔpH is necessary to induce other photoprotective mechanisms like the photosynthetic control of Cyt b_6f and the induction of light-harvesting complex stress-related protein 3 (LHCSR3) and PsbS that in turn dissipate excess energy at Photosystem II (PSII) as qE of non-photochemical quenching (NPQ) (3). As a next step, the activity of PGRL1-Fd-mediated CET is enhanced and contributes further to *pmf* (4). At this point, PGRL1-Fd-mediated CET possibly also replaces FDPs as the major AEF pathway. To balance *pmf*, ion channels in the thylakoid membrane either release cations (e.g. K^+, Mg^{2+} or Ca^{2+}) into the stroma or transport anions (e.g. $Cl^−$) into the lumen (5). A high electric potential (ΔΨ) would increase the probability of charge recombination and subsequently lead to photoinhibition (Davis *et al.*, 2016). After an extended period of HL (several min), ROS production at PSI leads to the activation of the true Mehler-reaction and subsequent water–water cycle (6), detoxifying ROS from the chloroplast and ultimately making FDPs redundant as electron sink. Furthermore, the reduced PQ-pool leads to the activation of the Stt7 kinase that phosphorylates LHCII, resulting in state-2 transition (7).

in the *pgr5* mutant is not significantly altered (Table S1), we cannot exclude the possibility that the lack of PGR5 effects the Ca^{2+}/CAS-dependent signalling, which in turn results in downregulation of the LHCSR3 expression. In future experiments, the *pgr5pgrl1* double mutant should be employed to fully confirm the nature of the different roles of PGR5 and PGRL1 under FL conditions.

In conclusion, our results provide compelling evidence for the fact that all three proteins, the FDPs, PGRL1 and PGR5 proteins, contribute to the survival of cells under FL, but to varying extents. The FDPs, PGRL1 and PGR5 pathways operate on different time-scales in the photoprotection of *C. reinhardtii* under FL. The presence of FDPs in the absence of PGR5, or the presence of PGR5 and PGRL1 in the absence of FDPs, is not sufficient to rescue the *C. reinhardtii* cells under harsh FL conditions. This situation suggests a clearly distinguishable, yet close, relationship between the function of the PGR5, PGRL1 and FDP proteins in photoprotection (Figure 7).

EXPERIMENTAL PROCEDURES

Chlamydomonas reinhardtii cells and growth conditions

The *C. reinhardtii* mutant strain *pgrl1*, its progenitor wt 137c and the *pgr5* mutant, its progenitor wt 137c and *pgr5* complemented strains were previously characterized (Dang *et al.*, 2014; Johnson *et al.*, 2014). The wt cc-4533 and FDP mutant lines, *flv* 208 (LMJ.RY0402.242208), *flv* 308 (LMJ.RY0402.229308) and *flv* 321 (LMJ.RY0402.052321) were purchased from the Chlamydomonas Research centre (www.chlamylibrary.org; Li *et al.*, 2016).

The *C. reinhardtii* wt strains and mutant lines were maintained under photoheterotrophic conditions in Tris/Acetate/Phosphate (TAP) medium (Gorman and Levine, 1965) at ambient air at 25°C under a continuous light intensity of 50 μmol photons m^{-2} sec^{-1} and under agitation (90 rpm). For preparing experimental *C. reinhardtii* cultures, the cells were harvested at OD750 = ~1.2, transferred to high-salt medium (HSM; Sueoka, 1960), diluted to OD750 = ~0.1 and cultivated photoautotrophically at ambient air and 25°C for 7 days at a continuous light intensity of 20 μmol photons m^{-2} sec^{-1} (CL 20), or at FL where 20 μmol photons m^{-2} sec^{-1} background light was interrupted every 5 min by 30-sec HL pulses with an intensity of 200 μmol photons m^{-2} sec^{-1} (mild FL, FL 20/200) or 600 μmol photons m^{-2} sec^{-1} (harsh FL, FL 20/600). The *pgr5* and *pgrl1* mutants originate from slightly different wt background; both strains belong to 137c ancestry; however, they have been cultivated for several decades separately. Growth analysis and comparison of several photosynthetic parameters of the cells growing in CL 20 and FL 20/200 conditions did not reveal a strong difference between the two wt 137c lines (Figure S7). Therefore, we selected the progenitor of *pgr5* as a reference strain for further analysis.

Immunoblot analysis

Total and membrane proteins were extracted, loaded on total protein basis, separated and immunoblotted as described in Jokel *et al.* (2015). For determination of PGR5, PsbA and PsaA proteins the membrane fractions were used. The antibodies against PSII (PsbA), PSI (PsaA), Cyt b_6f complex (Cyt *f*), FDX1, LHCSR3, Rubisco (RbcL), FeSOD and COXIIb were purchased from Agrisera,

Sweden. The PGR5 antibody was created by using an *A. thaliana* PGR5 peptide antigen (CDAKQRQGLIRLAKKNGER-NH2) conjugated with keyhole limpet haemocyanin (Agrisera, Sweden). As a secondary antibody, anti-rabbit horseradish peroxidase was used and visualized with ECL.

Fluorescence and P700 measurement with Dual-PAM 100

The Dual-PAM-100 fluorometer (Walz, Germany) and DUAL-K25 quartz cuvette were used for the simultaneous measurements of PSII and PSI parameters *in vivo*, based on Chl *a* fluorescence and the P700 absorbance changes (difference of intensities of 875 and 830 nm pulse-modulated measuring light reaching the photodetector), respectively (Baker, 2008; Klughammer and Schreiber, 2008). Before the measurements, the cells were transferred into fresh HSM and the Chl *a+b* concentration was adjusted to ~5 μg mL^{-1}. The cells were kept in the dark for 2–3 min before the FL-mimicking experiments. For mimicking FL with the DUAL-PAM-100, the actinic light intensity of 22 μmol photons m^{-2} sec^{-1} was disrupted every 5 min with 30 sec HL intensity of 210 μmol photons m^{-2} sec^{-1}. The following PSII and PSI parameters were determined: the maximum quantum yield of PSII, Fv/Fm = ($F_m - F_0$)/Fm; the effective PSII yield under actinic light, Y(II) = (Fm′ − F)/Fm′; the non-photochemical quenching, NPQ = (Fm − Fm′)/Fm′; the effective PSI yield under actinic yield, Y(I) = 1 − Y(ND) − Y(NA); the acceptor-side limitation of PSI, Y(NA) = (Pm − Pm′)/Pm; and the donor-side limitation of PSI, Y(ND) = P/Pm. P represents P700+ signal under actinic light. The maximum oxidizable P700, the Pm value, was measured by application of a saturating white-light pulse (4000 μmol photons m^{-2} sec^{-1}, duration 500 msec) on far-red light (75 W m^{-2}) background. The saturating pulse was regularly applied to measure the maximum fluorescence (Fm′) and maximum oxidizable P700 (Pm′) during actinic light illumination. For the calculation of Fv/Fm, the minimum (F_0) and maximum fluorescence (Fm) in the dark-adapted state were measured from cells kept for 45 min in darkness. For detection of the fast kinetics of the P700 oxido-reduction, 100 μg cells were filtered onto glass fibre discs (Millipore, USA) and dark-adapted for 45 min. The P700 signal was recorded by illumination with 1000 μmol photons m^{-2} sec^{-1} actinic light for 5 sec.

CONFLICT OF INTEREST

The authors have no conflict of interest to declare.

SUPPORTING INFORMATION

Additional Supporting Information may be found in the online version of this article.

Figure S1. Growth curves under constant illumination.

Figure S2. Verification of several *flvB* knockout lines.

Figure S3. NPQ of wt and mutant lines under different light conditions.

Figure S4. Fluorescence emission spectra at 77K.

Figure S5. TEM of *C. reinhardtii* cells.

Figure S6. Protein alignment of several FDPs.

Figure S7. Comparison of *C. reinhardtii* wt cultures.

Table S1. RNA-seq analysis of *pgrl1* and *pgr5* under FL 20/200 conditions

REFERENCES

Ahn, C.S., Lee, J.H., Reum Hwang, A., Kim, W.T. and Pai, H.-S. (2006) Prohibitin is involved in mitochondrial biogenesis in plants. *Plant J.* **46**, 658–667.

Allahverdiyeva, Y., Mustila, H., Ermakova, M., Bersanini, L., Richaud, P., Ajlani, G., Battchikova, N., Cournac, L. and Aro, E.M. (2013) Flavodiiron proteins Flv1 and Flv3 enable cyanobacterial growth and photosynthesis under fluctuating light. *Proc. Natl Acad. Sci. USA*, **110**, 4111–4116.

Allahverdiyeva, Y., Suorsa, M., Tikkanen, M. and Aro, E.M. (2015a) Photoprotection of photosystems in fluctuating light intensities. *J. Exp. Bot.* **66**, 2427–2436.

Allahverdiyeva, Y., Isojärvi, J., Zhang, P. and Aro, E.M. (2015b) Cyanobacterial oxygenic photosynthesis is protected by Flavodiiron proteins. *Life (Basel)*, **5**, 716–743.

Alric, J. (2010) Cyclic electron flow around photosystem I in unicellular green algae. *Photosynth. Res.* **106**, 47–56.

Alric, J. (2014) Redox and ATP control of photosynthetic cyclic electron flow in *Chlamydomonas reinhardtii*: involvement of the PGR5-PGRL1 pathway under anaerobic conditions. *Biochim. Biophys. Acta*, **1837**, 825–834.

Alric, J., Lavergne, J. and Rappaport, F. (2010) Redox and ATP control of photosynthetic cyclic electron flow in *Chlamydomonas reinhardtii*. *Biochim. Biophys. Acta*, **1797**, 44–51.

Armbruster, U., Labs, M., Pribil, M. *et al.* (2013) *Arabidopsis* CURVATURE THYLAKOID1 proteins modify thylakoid architecture by inducing membrane curvature. *Plant Cell*, **25**, 2661–2678.

Baker, N.R. (2008) Chlorophyll fluorescence: a probe of photosynthesis in vivo. *Annu. Rev. Plant Biol.* **59**, 89–113.

Bersanini, L., Battchikova, N., Jokel, M., Rehman, A., Vass, I., Allahverdiyeva, Y. and Aro, E.M. (2014) Flavodiiron protein Flv2/Flv4-related photoprotective mechanism dissipates excitation pressure of PSII in cooperation with phycobilisomes in cyanobacteria. *Plant Physiol.* **164**, 805–818.

Bersanini, L., Allahverdiyeva, Y., Battchikova, N., Heinz, S., Lespinasse, M., Ruohisto, E., Mustila, H., Nickelsen, J., Vass, I. and Aro, E.M. (2017) Dissecting the photoprotective mechanism encoded by the flv4-2 operon: a distinct contribution of Sll0218 in Photosystem II stabilization. *Plant, Cell Environ.* **40**, 378–389.

Cardol, P., Forti, G. and Finazzi, G. (2011) Regulation of electron transport in microalgae. *Biochim. Biophys. Acta*, **1807**, 912–918.

Chaux, F., Burlacot, A., Mekhalfi, M., Auroy, P., Blangy, S., Richaud, P. and Peltier, G. (2017a) Flavodiiron proteins promote fast and transient O$_2$ photoreduction in *Chlamydomonas*. *Plant Physiol.* **174**, 1825–1836.

Chaux, F., Johnson, X., Auroy, P., Beyly-Adriano, A., Te, I., Cuine, S. and Peltier, G. (2017b) PGRL1 and LHCSR3 compensate for each other in controlling photosynthesis and avoiding Photosystem I photoinhibition during high light acclimation of *Chlamydomonas* cells. *Mol. Plant*, **10**, 216–218.

Correa-Galvis, V., Redekop, P., Guan, K., Griess, A., Truong, T.B., Wakao, S., Niyogi, K.K. and Jahns, P. (2016) Photosystem II subunit PsbS is involved in the induction of LHCSR protein-dependent energy dissipation in *Chlamydomonas reinhardtii*. *J. Biol. Chem.* **291**, 17478–17487.

DalCorso, G., Pesaresi, P., Masiero, S., Aseeva, E., Schünemann, D., Finazzi, G., Joliot, P., Barbato, R. and Leister, D. (2008) A complex containing PGRL1 and PGR5 is involved in the switch between linear and cyclic electron flow in *Arabidopsis*. *Cell*, **132**, 273–285.

Dang, K.V., Plet, J., Tolleter, D. *et al.* (2014) Combined increases in mitochondrial cooperation and oxygen photoreduction compensate for deficiency in cyclic electron flow in *Chlamydomonas reinhardtii*. *Plant Cell*, **26**, 3036–3050.

Davis, G.A., Kanazawa, A., Schöttler, M.A. *et al.* (2016) Limitations to photosynthesis by proton motive force-induced photosystem II photodamage. *eLife*, **5**, e16921.

Finazzi, G. and Johnson, G.N. (2016) Cyclic electron flow: facts and hypotheses. *Photosynth. Res.* **129**, 227–230.

Finazzi, G. and Minagawa, J. (2015) High light acclimation in green microalgae. In *Non-photochemical Quenching and Thermal Energy Dissipation in Plants, Algae and Cyanobacteria* (Demmig-Adams, B., Garab, G., Adams III, W.W. and Govindjee, eds). Dordrecht: Springer, pp. 445–469.

Foyer, C.H. and Noctor, G. (2009) Redox regulation in photosynthetic organisms: signaling, acclimation, and practical implications. *Antioxid. Redox Signal.* **4**, 861–905.

Gerotto, C., Alboresi, A., Meneghesso, A., Jokel, M., Suorsa, M., Aro, E.M. and Morosinotto, T. (2016) Flavodiiron proteins act as safety valve for electrons in *Physcomitrella patens*. *Proc. Natl Acad. Sci. USA*, **113**, 12322–12327.

Gorman, D.S. and Levine, R.P. (1965) Cytochrome f and plastocyanin: their sequence in the photosynthetic electron transport chain of *Chlamydomonas reinhardtii*. *Proc. Natl Acad. Sci. USA*, **54**, 1665–1669.

Heinz, S., Rast, A., Shao, L. *et al.* (2016) Thylakoid membrane architecture in synechocystis depends on CurT, a homolog of the granal CURVATURE THYLAKOID1 Proteins. *Plant Cell*, **28**, 2238–2260.

Helman, Y., Tchernov, D., Reinhold, L., Shibata, M., Ogawa, T., Schwarz, R., Ohad, I. and Kaplan, A. (2003) Genes encoding A-type flavoproteins are essential for photoreduction of O$_2$ in cyanobacteria. *Curr. Biol.* **13**, 230–235.

Hertle, A.P., Blunder, T., Wunder, T., Pesaresi, P., Pribil, M., Armbruster, U. and Leister, D. (2013) PGRL1 is the elusive ferredoxin-plastoquinone reductase in photosynthetic cyclic electron flow. *Mol. Cell*, **49**, 511–523.

Horton, P., Ruban, A.V. and Walters, R.G. (1994) Regulation of light harvesting in green plants: indication by nonphotochemical quenching of chlorophyll fluorescence. *Plant Physiol.* **106**, 415–420.

Ilík, P., Pavlovič, A., Kouřil, R., Alboresi, A., Morosinotto, T., Allahverdiyeva, Y., Aro, E.-M., Yamamoto, H. and Shikanai, T. (2017) Alternative electron transport mediated by flavodiiron proteins is operational in organisms from cyanobacteria up to gymnosperms. *New Phytol.* **214**, 967–972.

Iluz, D., Alexandrovich, I. and Dubinsky, Z. (2012) The enhancement of photosynthesis by fluctuating light. In *Artificial Photosynthesis* (Najafpour, M., ed.). Rijeka: InTech, pp. 115–134.

Iwai, M., Takizawa, K., Tokutsu, R., Okamuro, A., Takahashi, Y. and Minagawa, J. (2010) Isolation of the elusive supercomplex that drives cyclic electron flow in photosynthesis. *Nature*, **464**, 1210–1213.

Jans, F., Mignolet, E., Houyoux, P.A., Cardol, P., Ghysels, B., Cuiné, S., Cournac, L., Peltier, G., Remacle, C. and Franck, F. (2008) A type II NAD(P)H dehydrogenase mediates light-independent plastoquinone reduction in the chloroplast of Chlamydomonas. *Proc. Natl Acad. Sci. USA*, **105**, 20546–20551.

Johnson, X., Steinbeck, J., Dent, R.M. *et al.* (2014) Proton gradient regulation 5-mediated cyclic electron flow under ATP- or redox-limited conditions: a study of ΔATpase pgr5 and ΔrbcL pgr5 mutants in the green alga *Chlamydomonas reinhardtii*. *Plant Physiol.* **165**, 438–452.

Jokel, M., Kosourov, S., Battchikova, N., Tsygankov, A.A., Aro, E.M. and Allahverdiyeva, Y. (2015) *Chlamydomonas* flavodiiron proteins facilitate acclimation to anoxia during sulfur deprivation. *Plant Cell Physiol.* **56**, 1598–1607.

Klughammer, C. and Schreiber, U. (2008) Saturation pulse method for assessment of energy conversion in PSI. *PAM Applic. Notes*, **1**, 11–14.

Kukuczka, B., Magneschi, L., Petroutsos, D., Steinbeck, J., Bald, T., Powikrowska, M., Fufezan, C., Finazzi, G. and Hippler, M. (2014) Proton gradient regulation5-like1-mediated cyclic electron flow is crucial for acclimation to anoxia and complementary to nonphotochemical quenching in stress adaptation. *Plant Physiol.* **165**, 1604–1617.

Li, X., Zhang, R., Patena, W. *et al.* (2016) An indexed, mapped mutant library enables reverse genetics studies of biological processes in *Chlamydomonas reinhardtii*. *Plant Cell*, **28**, 367–387.

Maruyama, S., Tokutsu, R. and Minagawa, J. (2014) Transcriptional regulation of the stress-responsive light harvesting complex genes in *Chlamydomonas Reinhardtii*. *Plant Cell Physiol.* **55**, 1304–1310.

Mosebach, L., Heilmann, C., Mutoh, R., Gäbelein, P., Steinbeck, J., Happe, T., Ikegami, T., Hanke, G., Kurisu, G. and Hippler, M. (2017) Association of Ferredoxin:NADP$^+$ oxidoreductase with the photosynthetic apparatus modulates electron transfer in *Chlamydomonas reinhardtii*. *Photosynth. Res.* **134**, 291.

Müller, P., Li, X.P. and Niyogi, K.K. (2001) Non-photochemical quenching. A response to excess light energy. *Plant Physiol.* **125**, 1558–1566.

Munekage, Y., Hojo, M., Meurer, J., Endo, T., Tasaka, M. and Shikanai, T. (2002) PGR5 is involved in cyclic electron flow around photosystem I and is essential for photoprotection in Arabidopsis. *Cell*, **110**, 361–371.

Niyogi, K.K. and Truong, T.B. (2013) Evolution of flexible non-photochemical quenching mechanisms that regulate light harvesting in oxygenic photosynthesis. *Curr. Opin. Plant Biol.* **16**, 307–314.

Peden, E.A., Boehm, M., Mulder, D.W., Davis, R., Old, W.M., King, P.W., Ghirardi, M.L. and Dubini, A. (2013) Identification of global ferredoxin interaction networks in *Chlamydomonas reinhardtii. J. Biol. Chem.* **288**, 35192–35209.

Peers, G., Truong, T.B., Ostendorf, E., Busch, A., Elrad, D., Grossman, A.R., Hippler, M. and Niyogi, K.K. (2009) An ancient light-harvesting protein is critical for the regulation of algal photosynthesis. *Nature*, **462**, 518–522.

Peltier, G., Tolleter, D., Billon, E. and Cournac, L. (2010) Auxiliary electron transport pathways in chloroplasts of microalgae. *Photosynth. Res.* **106**, 19–31.

Petroutsos, D., Terauchi, A.M., Busch, A., Hirschmann, I., Merchant, S.S., Finazzi, G. and Hippler, M. (2009) PGRL1 participates in iron-induced remodeling of the photosynthetic apparatus and in energy metabolism in *Chlamydomonas reinhardtii. J. Biol. Chem.* **284**, 32770–32781.

Petroutsos, D., Busch, A., Janssen, I., Trompelt, K., Bergner, S.V., Weinl, S., Holtkamp, M., Karst, U., Kudla, J. and Hippler, M. (2011) The chloroplast calcium sensor CAS is required for photoacclimation in *Chlamydomonas reinhardtii. Plant Cell*, **23**, 2950–2963.

Petroutsos, D., Tokutsu, R., Maruyama, S. *et al.* (2016) A blue-light photoreceptor mediates the feedback regulation of photosynthesis. *Nature*, **537**, 563–566.

Schneider, D., Berry, S., Rich, P., Seidler, A. and Rögner, M. (2001) A regulatory role of the PetM subunit in a cyanobacterial cytochrome b6f complex. *J. Biol. Chem.* **276**, 16780–16785.

Shikanai, T. (2014) Central role of cyclic electron transport around photosystem I in the regulation of photosynthesis. *Curr. Opin. Biotechnol.* **26**, 25–30.

Shikanai, T. and Yamamoto, H. (2017) Contribution of cyclic and pseudocyclic electron transport to the formation of proton motive force in chloroplasts. *Mol. Plant.* **10**, 20–29.

Shimakawa, G., Ishizaki, K., Tsukamoto, S., Tanaka, M., Sejima, T. and Miyake, C. (2017) The liverwort *Marchantia* drives alternative electron flow using a flavodiiron protein to protect PSI. *Plant Physiol.* **173**, 1636–1647.

Steinbeck, J., Nikolova, D., Weingarten, R., Johnson, X., Richaud, P., Peltier, G., Hermann, M., Magneschi, L. and Hippler, M. (2015) Deletion of proton gradient regulation 5 (PGR5) and PGR5-like 1 (PGRL1) proteins promote sustainable light-driven hydrogen production in Chlamydomonas reinhardtii due to increased PSII activity under sulfur deprivation. *Front. Plant Sci.* **6**, 892.

Sueoka, N. (1960) Mitotic replication of deoxyribonucleic acid in *Chlamydomonas reinhardtii. Proc. Natl Acad. Sci. USA*, **46**, 83–91.

Suorsa, M., Järvi, S., Grieco, M. *et al.* (2012) PROTON GRADIENT REGULATION5 is essential for proper acclimation of *Arabidopsis* photosystem I to naturally and artificially fluctuating light conditions. *Plant Cell*, **24**, 2934–2948.

Takahashi, H., Clowez, S., Wollman, F.A., Vallon, O. and Rappaport, F. (2013) Cyclic electron flow is redox-controlled but independent of state transition. *Nat. Commun.* **4**, 1954–1961.

Terashima, M., Petroutsos, D., Hudig, M. *et al.* (2012) Calcium-dependent regulation of cyclic photosynthetic electron transfer by a CAS, ANR1, and PGRL1 complex. *Proc. Natl Acad. Sci. USA*, **109**, 17717–17722.

Tikkanen, M., Grieco, M., Kangasjärvi, S. and Aro, E.M. (2010) Thylakoid protein phosphorylation in higher plant chloroplasts optimizes electron transfer under fluctuating light. *Plant Physiol.* **152**, 723–735.

Tiwari, A., Mamedov, F., Grieco, M., Suorsa, M., Jajoo, A., Styring, S., Tikkanen, M. and Aro, E.M. (2016) Photodamage of iron–sulphur clusters in photosystem I induces non-photochemical energy dissipation. *Nat. Plants*, **2**, 16035.

Tolleter, D., Ghysels, B., Alric, J. *et al.* (2011) Control of hydrogen photoproduction by the proton gradient generated by cyclic electron flow in *Chlamydomonas reinhardtii. Plant Cell*, **23**, 2619–2630.

Vicente, J.B., Gomes, C.M., Wasserfallen, A. and Teixeira, M. (2002) Module fusion in an A-type flavoprotein from the cyanobacterium *Synechocystis* condenses a multiple component pathway in a single polypeptide chain. *Biochem. Biophys. Res. Commun.* **294**, 82–87.

Wada, S., Yamamoto, H., Suzuki, Y., Yamori, W., Shikanai, T. and Makino, A. (2018) Flavodiiron protein substitutes for cyclic electron flow without competing CO_2 assimilation in rice. *Plant Physiol.* **176**, 1509–1518.

Wasserfallen, A., Ragettli, S., Jouanneau, Y. and Leisinger, T. (1998) A family of flavoproteins in the domains Archaea and Bacteria. *Eur. J. Biochem.* **254**, 325–332.

Wobbe, L., Blifernez, O., Schwarz, C., Mussgnug, J.H., Nickelsen, J. and Kruse, O. (2009) Cysteine modification of a specific repressor protein controls the translational status of nucleus-encoded LHCII mRNAs in *Chlamydomonas. Proc. Natl Acad. Sci. USA*, **106**, 13290–13295.

Yamamoto, H., Takahashi, S., Badger, M.R. and Shikanai, T. (2016) Artificial remodelling of alternative electron flow by Flavodiiron proteins in *Arabidopsis. Nat. Plants*, **2**, 16012.

Yeremenko, N., Jeanjean, R., Prommeenate, P., Krasikov, V., Nixon, P.J., Vermaas, W.F., Havaux, M. and Matthijs, H.C. (2005) Open reading frame ssr2016 is required for antimycin A-sensitive photosystem I driven cyclic electron flow in the cyanobacterium *Synechocystis* sp. PCC 6803. *Plant Cell Physiol.* **46**, 1433–1436.

Zhang, P., Allahverdiyeva, Y., Eisenhut, M. and Aro, E.M. (2009) Flavodiiron proteins in oxygenic photosynthetic organisms: photoprotection of photosystem II by Flv2 and Flv4 in *Synechocystis* sp. PCC 6803. *PLoS ONE*, **4**, e5331.